A rapid way to synthesize magnesium whitlockite microspheres for high efficiency removing heavy metals

Chucheng Lin[a], Yueyue Wang[b],*, Yang Zhou[c], Yi Zeng[a],*

[a]*State Key Laboratory of High Performance Ceramics and Superfine Microstructure, Shanghai Institute of Ceramics, Chinese Academy of Sciences, Shanghai 200050, China, Tel. +86-21-52411020, emails: zengyi@mail.sic.ac.cn (Y. Zeng), chucheng@mail.sic.ac.cn (C.C. Lin)*
[b]*College of Materials Science and Engineering, Taiyuan University of Technology, Taiyuan 030024, China, Tel. +86-351-6010540, email: wangyueyue@tyut.edu.cn*
[c]*Biomaterials and Tissue Engineering Research Center Shanghai Institute of Ceramics, Chinese Academy of Sciences, Shanghai 200050, China, Tel. +86-21-52412810, email: zhouyang_1990@126.com*

ABSTRACT

Magnesium whitlockite has been widely applied in many fields, such as protein adsorption and drug delivery. However, the application of MWH in heavy metal adsorption has not been reported yet. To obtain the adsorbents with high adsorption capacity, we developed a rapid way to synthesize magnesium whitlockite microspheres with nano-pores by microwave hydrothermal method using the adenosine 5'-triphosphate disodium salt hydrate as a phosphorus source. The effects of the reaction time and temperature on the composition and morphology of magnesium whitlockite were investigated. Heavy metal removal ability of the prepared magnesium whitlockite at different adsorption time and initial Pb^{2+} concentration was studied. The results showed that the reaction temperature and time did not have an obvious effect on the microstructure of the prepared MWH. They were about 300 nm in diameter with rough surfaces. Adsorption studies showed that Pb^{2+} ions could be adsorbed remarkably and efficiently by the prepared MWH. The adsorption equilibrium of MWH in Pb^{2+} solution (200 mg L^{-1}) could be reached in 5 min. The adsorption kinetic study showed that it obeyed the pseudo-second-order kinetic model and the Langmuir isotherm model. The experimental maximum adsorption capacity of the prepared MWH was 2311 mg L^{-1}. Furthermore, the remove percentage of Cd^{2+}, Cu^{2+} and Pb^{2+} ions by the MWH in a mixed solution containing these metal ions were 22.3%, 21.2%, and 86.4%, respectively, indicating that the prepared MWH had an ability to electively adsorb Pb^{2+} ions in Cd^{2+}, Cu^{2+}, and Pb^{2+}-containing solution. Therefore, the prepared magnesium whitlockite is a promising adsorbent for being used in the treatment of water pollution.

Keywords: Magnesium whitlockite; Heavy metals; Selective adsorption; Water pollution

1. Introduction

Water is one of the most important and essential resources for living beings on the earth [1,2]. Unfortunately, water pollution by heavy metal ions is getting more and more deteriorated due to rapid industrialization and urbanization. Some heavy metals, such as Pb^{2+}, Cd^{2+} and Cu^{2+} ions, are notorious water contaminants with serious side effects and high toxicity even at low concentrations [3–5]. Therefore, the efficient and rapid removal of toxic heavy metal ions from aqueous solution is an urgent need for public health and environmental ecosystems. Over the decades, several methods have been developed and employed for removing heavy metals including electrolysis, precipitation, ultrafiltration and adsorption [2,6]. Among these methods, the

* Corresponding authors.

adsorption is considered as the most suitable solution owing to its advantages of easy operation and wide applicability [7,8]. Therefore, there is an urgent need to develop highly efficient and cost-effective adsorbents for removing heavy mental ions from polluted water.

In recent years, the adsorption of heavy metals by inorganic components of hard tissues, which are abundant in nature, has attracted much attention. For example, there are many reports about the application of hydroxyapatite ($Ca_{10}(PO_4)_6(OH)_2$), the main mineral component of animal hard tissues, in heavy metal adsorption [9]. Liao et al. [10] explored the ability of carbonate hydroxyapatite to remove lead ions (Pb^{2+}), and the maximum adsorption capacity of Pb^{2+} ions was 101 mg g^{-1}. It is likely that the large specific surface area endows the nano-calcium phosphate materials with an ability to adsorb heavy metals effectively [11]. To obtain the adsorbents with high adsorption capacity, nano-sized adsorbents have been developed for the removal of the heavy mental ions. Zhao et al. [12] synthesized hydroxyapatite nanosheet-assembled microspheres with a high adsorption capacity of heavy metal ions. Wang et al. [13] prepared flower-like hydroxyapatite to selectively adsorb Pb^{2+} ions. Zhang et al. [14] investigated the effectiveness and mechanism of immobilization of Pb^{2+} and Cd^{2+} ions on the nano-hydroxyapatite particles. Magnesium whitlockite ($Ca_{18}Mg_2(HPO_4)_2(PO_4)_{12}$, MWH), which is formed by partial replacement of calcium with magnesium, is the second most abundant mineral in hard tissues. However, there are few reports on the adsorption properties and mechanism of heavy metals in MWH, due to the difficulty in synthesizing single-phase MWH materials [15,16]. Previous studies have shown that the MWH exhibited a high protein-adsorption capacity, exhibiting a promising application in protein adsorption [17]. Therefore, we hypothesize that the MWH with large specific surface area might have high ion-adsorption capacity.

Since adenosine triphosphate (ATP) is usually recognized as a template and can modulate the formation of hierarchical nanostructures [18], we reported a rapid way to synthesize magnesium whitlockite with nano-pores by microwave hydrothermal method using the adenosine 5'-triphosphate disodium salt hydrate (Na_2ATP) as a phosphorus source. We investigated the effects of reaction time and temperature on the composition and morphology of MWH. Then we studied the effects of contact time and initial Pb^{2+} concentration on heavy metal adsorption ability of the prepared MWH. Furthermore, the adsorption kinetic and isotherm of MWH were explored. The experimental results confirmed that the prepared MWH had a high and efficient adsorption ability for heavy metal ions, holding a promising application as an adsorbent in water pollution.

2. Experimental

2.1. Preparation of MWH microspheres

The MWH microspheres were synthesized by a microwave hydrothermal method. In a typical procedure, 0.110 g adenosine Na_2ATP was slowly added into a mixed solution containing 7 mL $CaCl_2$ solution (0.1 M), 3 mL $MgCl_2$ solution (0.1 M) and 30 mL deionized water with magnet stirring at room temperature. The pH of the solution was adjusted to 9

by addition of NaOH (1 M) aqueous solution. The obtained solution was placed into a 60 mL polytetrauoroethylene auto-clave, sealed and microwave-heated in a microwave oven with frequency 2.45 GHz, maximum power 1,000 W (MDS-6, Sineo, China) at 120°C for 10 min. After reaction, the powders were collected by centrifugation, washed with deionized water and ethanol for three times, and then dried at 60°C for 12 h before further uses. In addition, in order to investigate the effect of the reaction condition on the microstructure of the samples, experiments with varied reaction time and temperature were carried out, and the detailed experimental parameters were listed in Table 1.

2.2. Adsorption experiments

All the adsorption experiments were carried out at room temperature. The Pb^{2+} solutions were obtained by dissolving $Pb(NO_3)_2$ in deionized water. The pH values of the Pb^{2+} solutions were adjusted to 5.5 by adding either HCl or $NH_3 \cdot H_2O$ aqueous solution. The adsorption kinetic studies were carried out as follows: The MWH (10 mg) powders were added into 20 mL of 200 mg L^{-1} Pb^{2+} solution under magnet stirring. After 5, 10, 20, 40, and 60 min, 1 mL medium was collected and centrifuged at 8,000 rpm for 10 min. The supernatant was analyzed by inductively coupled plasma-optical emission spectrometry (ICP). The adsorption capacity q_t (mg g^{-1}) at t (min) was calculated according to the following equation [19]:

$$q_t = \frac{(C_0 - C_t)}{m} \times V \tag{1}$$

where C_0 and C_t are the concentration of Pb^{2+} ions at the 0 and t min in solution (mg L^{-1}), respectively; V is the volume of the Pb^{2+} solution (L), and m is the dosage of the sorbent (mg). In order to evaluate the adsorption equilibrium of Pb^{2+} on the MWH powders, 10 mg samples were immersed into 20 mL of Pb^{2+} solution with initial concentrations of 500; 1,000; 1,500; 2,000; and 2,500 mg L^{-1} for 1 h under magnet stirring. After that, the slurries were separated by centrifugation and the supernatant was analyzed by ICP.

The selective adsorption ability of the prepared MWH was also investigated using a mixed solution containing Pb^{2+}, Cu^{2+}, and Cd^{2+}. The mixed solution was prepared by dissolving $Cu(NO_3)_2 \cdot 3H_2O$, $Pb(NO_3)_2$ and $CdCl_2 \cdot 2.5H_2O$ in deionized water. The initial concentration of each heavy metal ions was 200 mg L^{-1}. The MWH samples (10 mg) were immersed into 20 mL mixed solution for 1 h, and then the slurries

Table 1
Preparation conditions of different samples by microwave hydrothermal method

Sample number	Temperature (°C)	Time (min)
MWH-1	120	10
MWH-2	120	60
MWH-3	140	10
MWH-4	160	10
MWH-5	180	10

were separated by centrifugation and the supernatant was analyzed by ICP.

In addition, in order to evaluate the adsorption efficiency of the prepared MWH, the hydroxyapatite (HAP) powder synthesized according to a previous study [20] was used as the control group. The process of adsorption experiment on HAP is exactly the same as that of MWH.

2.3. Characterization

The X-ray diffractometer (XRD, Rigaku D/max 2,550 V; Cu Ka1 radiation) and Fourier transform infrared spectroscopy (FTIR, Thermo Nicolet-nexus, USA) were employed to characterize the composition of the samples. The morphology and chemical composition of the samples were characterized by scanning electron microscope (SEM, FEI Magellan 400, USA) equipped with energy dispersive X-ray spectrometry (EDX), field emission scanning electron microscopy (FESEM, JSM-6700F, JEOL, Japan) and transmission electron microscope (TEM, JEM-2100F, JEOL, Japan). The concentration of heavy mental ions were measured by (ICP, Varain 715-ES, USA). The thermogravimetric (TG) curves were measured at the heating rate of $10°C\ min^{-1}$ in air on a STA 409/PC simultaneous thermal analyzer (Netzsch, Germany). Brunauer–Emmett–Teller (BET, V-sorb 2800P, Gold APP, China) was employed to measure the surface area and pore volume.

3. Results and discussion

3.1. Characterization of the MWH microspheres

The samples were rapidly synthesized by a microwave hydrothermal method, in which ATP was used to supply PO_4^{3-} ions. XRD was employed to identify the phase composition of the synthesized powders under different conditions and the results are shown in Fig. 1. The diffraction pattern of MWH-1 shows an amorphous phase with no obvious diffraction peaks. After prolonging the reaction time (MWH-2), diffraction peaks which agreed with the standard diffraction peaks of MWH (JCPDS 09-0169) were

observed [17], due to the crystallization of the amorphous particles. It could be clearly observed that the peak intensity gradually increased with the increase of the reaction temperature (MWH-3 ~ MWH-5), indicating the high microwave-heated temperature could result in well-crystallized MWH powders.

The FTIR spectra of the synthesized samples are shown in Fig. 2. The absorption bands at around 3,421 and 1,634 cm^{-1} were ascribed to the adsorbed water. The absorption peaks at around 563 (v4), 605 (v4), 1,033 (v3) cm^{-1} were assigned to the PO_4^{3-} stretching bands [21]. The peak signals of PO_4^{3-} at around 563 and 605 cm^{-1} became stronger as the microwave hydrothermal temperature increased, which was consistent with the XRD results. Both XRD and FTIR results confirmed that the synthesized powders were pure magnesium whitlockite, and the MWH were not well-crystallized at low microwave hydrothermal temperature and short reaction time.

The morphologies of the obtained samples were characterized by SEM and TEM and the results are shown in Fig. 3. It could be observed that the diameter of the prepared magnesium whitlockite microspheres were about 300 nm. There were lot of nanoparticles located on the surface of the microspheres, resulting in a relatively rough surface structure. SEM images showed that there was no obvious difference among the morphology of samples prepared under different reaction conditions. However, TEM images showed that there was a lot of nano-pores in the microspheres of sample MWH-1 (Fig. 3b). After prolonging the reaction time to 1 h, the nano-pores drastically reduced and the MWH-2 became solid microspheres (Fig. 3d). When the microwave hydrothermal temperature increased to above 140°C, the number of nano-pores was much lower than that of 120°C. This indicated that the high temperature and long reaction time could lead to the formation of solid microspheres. According to these data, the MWH microspheres could be rapidly synthesized by microwave hydrothermal method, and the degree of crystallization and nano-pores formation could be controlled by adjusting the reaction time and temperature.
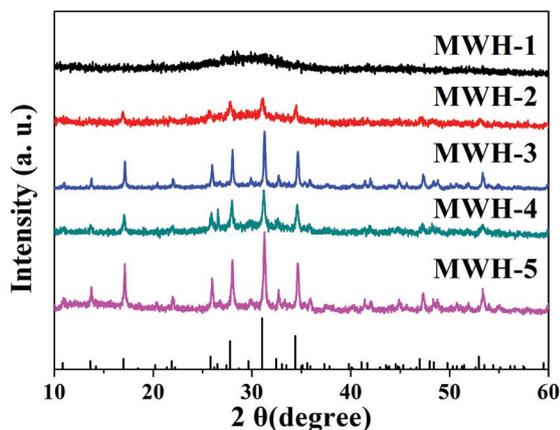

Fig. 1. XRD data of the synthesized samples. MWH-1: 120°C for 10 min; MWH-2: 120°C for 60 min; MWH-3: 140°C or 10 min; MWH-4: 160°C or 10 min; MWH-5:180°C or 10 min.
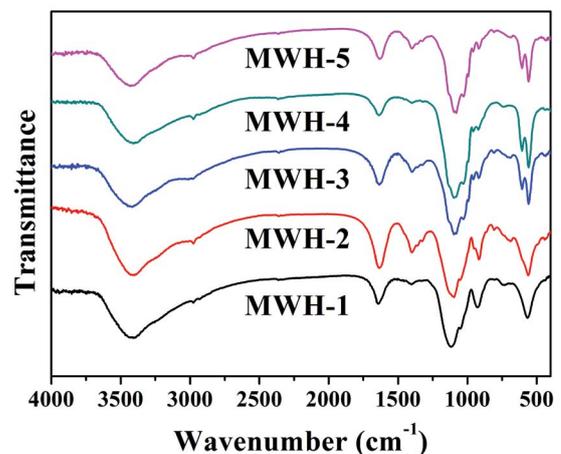

Fig. 2. FTIR patterns of the synthesized samples. MWH-1: 120°C for 10 min; MWH-2: 120°C for 60 min; MWH-3: 140°C or 10 min; MWH-4: 160°C or 10 min; MWH-5:180°C or 10 min.
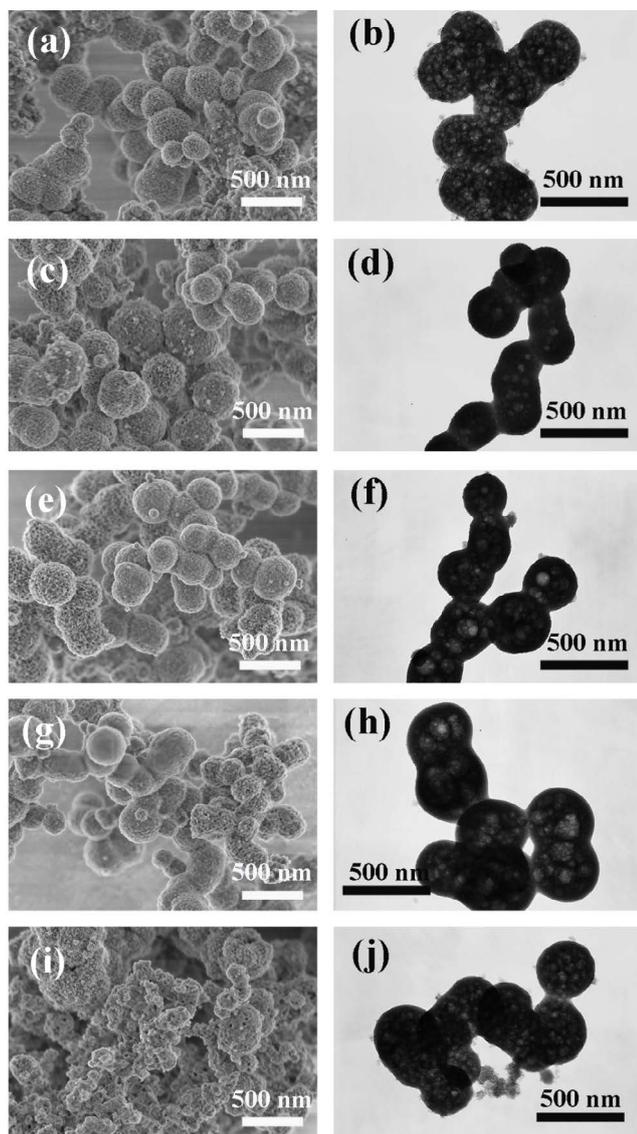
Fig. 3. SEM (left column) and TEM (right column) images of the synthesized samples. (a,b) MWH-1: 120°C for 10 min; (c,d) MWH-2: 120°C for 60 min; (e,f) MWH-3: 140°C or 10 min; (g,h) MWH-4: 160°C or 10 min; and (i,j) MWH-5:180°C or 10 min.
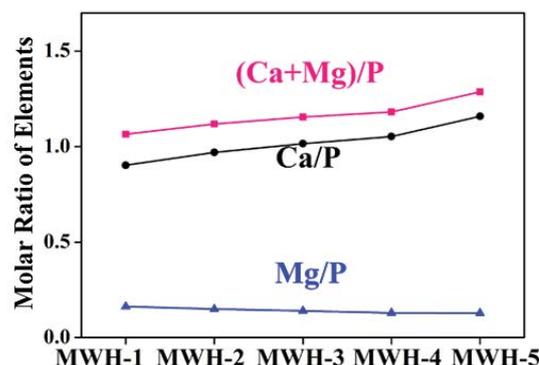

Fig. 4. ICP results of the synthesized samples. MWH-1: 120°C for 10 min; MWH-2: 120°C for 60 min; MWH-3: 140°C or 10 min; MWH-4: 160°C or 10 min; MWH-5:180°C or 10 min.

method. The high microwave hydrothermal temperature and long reaction time could contribute to produce more PO_4^{3-} ions and driving force for nucleation, resulting in crystallization.

Furthermore, we also investigated the stability of the MWH powders by TG analysis and the results were showed in Fig. 5. The weight loss of the samples from 30°C to 150°C was mainly contributed to the water evaporation [22]. The sample MWH-1 exhibited a weight loss of 11.82% from 30°C to 150°C, while the weight loss of MWH-4 and MWH-5 were 5.63% and 2.68%, respectively. After this stage, the mass loss of MWH-1 continuously increased with the increase of temperature, and finally reached 33.95% at 900°C, which was much higher than that of the other samples. The reasons for the weight loss of MWH-1 were the adsorbed water, bounded water and the amorphous phase [17]. Therefore, the crystallized MWH powders was more stable than the amorphous MWH-1.

3.2. Adsorption performance studies

According to previous studies [14,23,24], the high specific surface area or porous structure and poor-crystallinity could improve the adsorption capacity of adsorbents for heavy metals. Therefore, the amorphous MWH-1 with lots

In order to identify the chemical composition of the MWH microspheres, a certain amount of samples were dissolved and the concentrations of Ca, Mg, and P ions in the solution were analyzed by ICP. The element molar ratios of the prepared samples are shown in Fig. 4. The (Ca + Mg)/P of amorphous phase MWH-1 was a bit lower than that of crystallized MWH-5. There were no significant differences in the composition of these powders. Moreover, the (Ca + Mg)/P element molar ratio of MWH powders were close to that of standardized MWH powder $(Ca_{18}Mg_2(HPO_4)_2(PO_4)_{12})$ with (Ca + Mg)/P of 1.428. The results showed that the microwave hydrothermal temperature and reaction time had little influence on the composition of the MWH powders. Based on the above results, we developed a simple and rapid way to prepare the MWH microspheres by a microwave hydrothermal
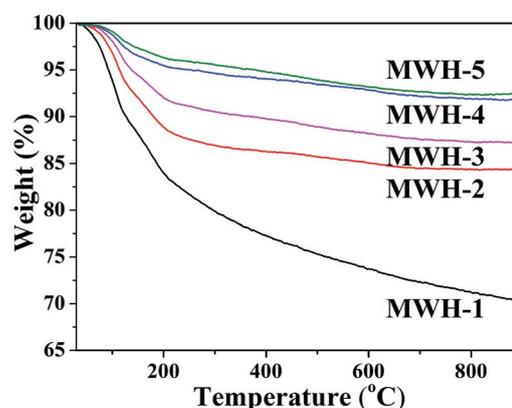

Fig. 5. TG curves of the synthesized samples. MWH-1: 120°C for 10 min; MWH-2: 120°C for 60 min; MWH-3: 140°C or 10 min; MWH-4: 160°C or 10 min; MWH-5:180°C or 10 min.

of nano-pores was used to remove the heavy metal ions for potential application in water treatment. The surface area of MWH-1 was 44.6 m^2 g^{-1}. The average pore diameter and cumulative pore volume were 7.2 nm and 0.11 cm^3 g^{-1}, respectively. To evaluate the adsorption ability of the MWH, the hydroxyapatite was served as a control group, since hydroxyapatite is an effective candidate to adsorb heavy metal ions. Subsequently, adsorption isotherms of the MWH and HAP for removing Pb^{2+} ions were investigated by a series of experiments. Fig. 6 shows the effect of the contact time on the Pb^{2+} ions adsorption. At the initial Pb^{2+} concentration of 200 mg L^{-1}, both MWH and HAP could quickly reach the adsorption equilibrium at 5 min. The adsorption amount of Pb^{2+} ions onto the MWH and HAP at adsorption equilibrium were 331.8 and 128.3 mg g^{-1}, respectively. It was obvious that the equilibrium adsorption capacity of MWH was about three times higher than that of HAP. Furthermore, the removal percentage of Pb^{2+} ions by MWH and HAP within 1 h were 99.1% and 38.2%, respectively. The results demonstrated that the MWH could efficiently remove heavy metals in a short time.

The kinetic order of the adsorption process was also explored through studying the kinetic order model. A lot of studies have reported that the HAP agree with the pseudo-second-order model. Therefore, it is necessary to study whether MWH obey the pseudo-second-order model. The pseudo-second-order model is as below [25]:

$$\frac{t}{q_t} = \frac{1}{kq_e^2} + \frac{t}{q_e} \qquad (2)$$

In which q_t is the adsorption capacity of Pb^{2+} at t (min) and q_e is the equilibrium adsorption amount (mg g^{-1}), k is the second-order rate constant (g mg^{-1} min^{-1}). The slope of $1/q_e$ is obtained by plotting t/q_t versus t.

The correlation coefficient R^2 of the pseudo-second-order model is shown in Fig. 7. Our results showed that the R^2 values of MWH and HAP were close to 1, suggesting that the adsorption process of Pb^{2+} ions on the MWH and HAP agreed with the pseudo-second-order kinetic model [26].
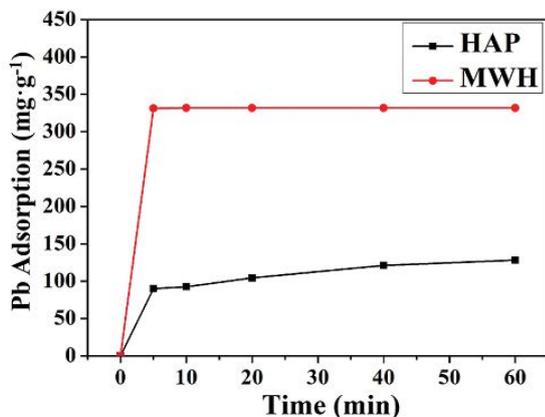

Fig. 6. Adsorption of Pb^{2+} ions with different contact time of the samples.
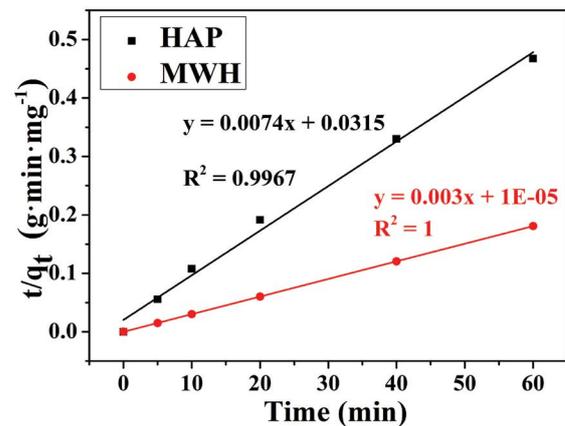

Fig. 7. The pseudo-second-order adsorption kinetic plots for Pb^{2+} ions of the samples.

According to the plot of pseudo-second-order kinetic model, the calculated q_e values of MWH and HAP were 333.3 and 135.1 mg g^{-1}, respectively. Under the same conditions, the equilibrium adsorption amount of our experiment results were 331.8 and 128.3 mg g^{-1}, which were very close to the calculated q_e values. These results indicated that the equilibrium adsorption of the MWH and HAP could nearly complete within 1 h. The adsorption process of Pb^{2+} ions on the MWH and HAP might follow the pseudo-second-order kinetic model.

The adsorption isotherms of the MWH and HAP adsorbents were explored by changing the initial concentrations of Pb^{2+} ions from 500 to 2,500 mg L^{-1}. The experimental results from the different initial concentrations were fitted with well-known Langmuir isotherm model equation [27]:

$$\frac{C_e}{q_e} = \frac{C_e}{q_m} + \frac{1}{k_L q_m} \qquad (3)$$

In which C_e (mg L^{-1}) and q_e (mg g^{-1}) are the equilibrium concentration and capacity of Pb^{2+} ions adsorption, respectively. The q_m (mg g^{-1}) represents the maximum adsorption capacity of Pb^{2+} ions, k_L (L mg^{-1}) represents the Langmuir constant, indicating the relative strength of adsorption.

The results according to the Langmuir isotherm model equation are shown in Fig. 8. It could be seen that the correlation coefficients R^2 of Langmuir isotherm model for MWH and HAP adsorbent were 0.9779 and 0.9609, respectively, suggesting that the adsorption process of MWH and HAP could be suitable for Langmuir isotherm model. It is known that the Langmuir model is based on the assumption of uniform surface properties in the adsorbent [28]. Therefore, the MWH with lots of nano-pores could provide more uniform adsorption sites than that of HAP. The calculated maximum adsorption capacity of Pb^{2+} ions on the MWH and HAP from Langmuir isotherm equation were 2,500 and 1,250 mg g^{-1}, respectively, while the experimental maximum adsorption capacity of Pb^{2+} ions on the MWH and HAP were 2,311 and 1,007 mg g^{-1}, respectively. The calculated results were consistent with the experimental

data, indicating the applicability of Langmuir isotherm model. Moreover, the adsorption capacity of MWH in our study was much greater than that of HAP. The maximum adsorption capacities of Pb^{2+} ions on HAP in previous studies were showed in Table 2. It could be clearly observed that the adsorption capacity of Pb^{2+} ions on MWH was much higher than the other materials. 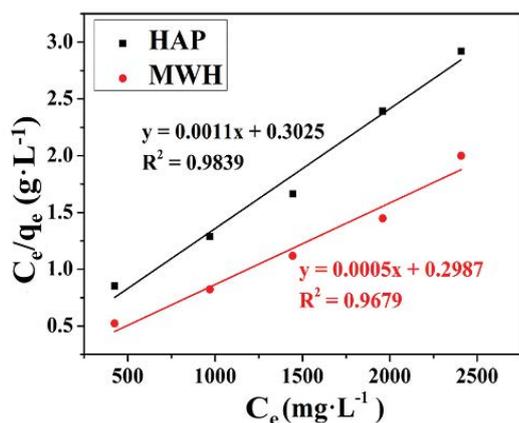It is well known that HAP has been confirmed as an effective adsorption material due to the ion exchange reaction and physical adsorption [13,29]. The amorphous phase of MWH may promote ion exchange reaction owing to the poor crystallinity [23]. On the other hand, the MWH was formed by the substitution of calcium ions with the magnesium ions, which may also contribute to the ion exchange reaction. In addition, the MWH microspheres with nano-pores also provided more physical adsorption sites for adsorption of heavy metal ions. Taken together, the results showed the amorphous MWH with nano-pores could significantly improve the removal of Pb^{2+} ions, and MWH might serve as an efficient and potential adsorbent for the adsorption of Pb^{2+} ions in aqueous solution.

In order evaluate the adsorption mechanism of the prepared MWH, the samples immersed in Pb^{2+} solution of 2,500 mg L^{-1} for 1 h were analyzed by SEM, EDX and FTIR. The microstructure and EDX mapping of the MWH after absorbing Pb^{2+} for 1 h were showed in Fig. 9. It could be observed that there were some newly formed small particles. In addition, the surface of the powder turned from nanopores to smooth structure, indicating that there was new substance formed in the surface of the powder. The EDX mapping analysis showed that the powders were composed of Pb, Ca, P, and O and they uniformly distributed in the samples after adsorbing. These results indicated that adsorption of lead ions from solution might be through surface ion exchange.

Fig. 8. Langmuir adsorption isotherm for Pb^{2+} ions of the samples.

Table 2
Summary of the maximum adsorption Pb^{2+} capacities on different adsorbents

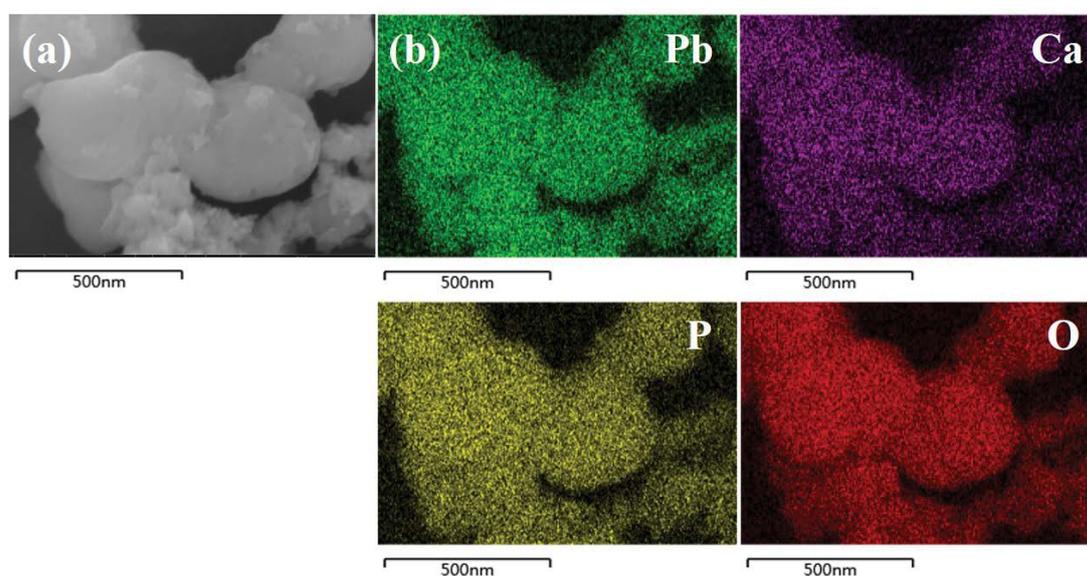| Adsorbent	Initial concentration (mg L^{-1})	Adsorption capacity q_m (mg g^{-1})	Reference
Carbonate hydroxyapatite	10–500	101	[10]
Hydroxyapatite	1,000–8,000	320	[8]
Carbonated hydroxyapatite/chitosan	400	559.6	[30]
Magnesium whitlockite	500–2,500	2,311	Present study

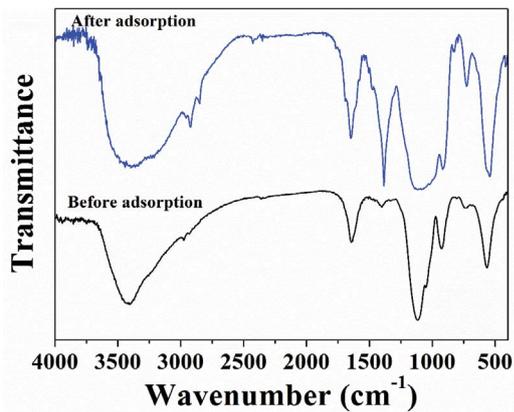Fig. 9. SEM (a) and EDX mapping (b) images of MWH after soaked in Pb^{2+} solution for 1 h.

Fig. 10. FTIR spectrum of MWH before and after soaked in Pb²⁺ solution for 1 h.
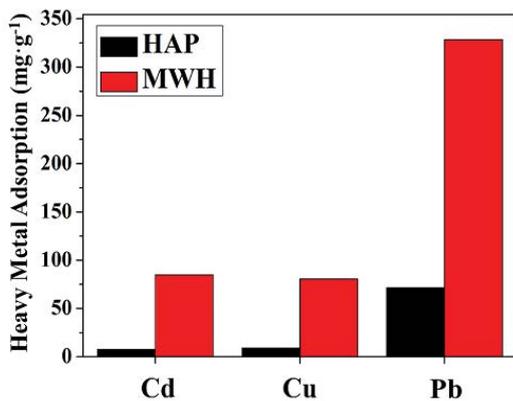

Fig. 11. Selective adsorption activities of the samples for heavy metal ions.

The FTIR spectrum of MWH after adsorption of Pb^{2+} is displayed in Fig. 10. It could be observed that there was no obvious difference between the displacement of infrared absorption peaks before and after adsorption of Pb^{2+} ions. This further confirmed that the adsorption of Pb^{2+} was mainly ascribed to the substitution of cations in MWH [30–32].

The selective adsorption activities of heavy metal ions on the MWH and HAP were also investigated in the solution containing heavy metal ions of Cd^{2+}, Cu^{2+}, and Pb^{2+} ions. The whole adsorption process lasted for about 1 h. The results of the selective adsorption are presented in Fig. 11. The adsorption values of Cd^{2+}, Cu^{2+}, and Pb^{2+} ions on the MWH at 1 h were 84.6, 80.5, and 328.4 mg g⁻¹, respectively, and the adsorption efficiencies of Cd^{2+}, Cu^{2+}, and Pb^{2+} ions on the MWH were 22.3%, 21.2%, and 86.4%, respectively. Both the adsorption values and efficiencies of Cd^{2+}, Cu^{2+}, and Pb^{2+} ions on the MWH were much higher than that of the HAP. Additionally, these results also indicated that the adsorption of Pb^{2+} ions was more active than those of the Cd^{2+} and Cu^{2+} ions onto the MWH and HAP. According to the previous studies [33], the adsorption efficiency mainly depends on the interaction force between the adsorbent material and metal ions. Therefore, the highest adsorption value of Pb^{2+} ions on the MWH and HAP might be due to

the stronger interaction force between lead ion and MWH than other metal ions.

4. Conclusions

In summary, we reported a rapid way to synthesize magnesium whitlockite microspheres with nano-pores by microwave hydrothermal method using the adenosine Na_2ATP as a phosphorus source. The microwave-heated time and temperature did not have an obvious effect on the phase composition and morphology of the prepared MWH. The amorphous MWH with nano-pores showed a relatively high adsorption capacity for Pb^{2+} ions. The adsorption kinetic of Pb^{2+} ions on the MWH adsorbents agreed well with the pseudo-second-order kinetic. The adsorption isotherm of the MWH for Pb^{2+} ions obeyed the Langmuir isotherm model. Furthermore, the MWH had an ability to selectively adsorb Pb^{2+} ions in Cd^{2+}, Cu^{2+} and Pb^{2+}-containing solution. The results suggest that the prepared MWH with rapid preparation method and strong adsorption capacity can be used as an ideal adsorbent for removing heavy metal ions as Pb^{2+} in water.

References

[1]   T.A.K. Sandhya Babel, Low-cost adsorbents for heavy metals uptake from contaminated water: a review, J. Hazard. Mater., 97 (2003) 219–243.
[2]   I. Ali, New generation adsorbents for water treatment, Chem. Rev., 112 (2012) 5073–5091.
[3]   C. Zhu, Z. Luan, Y. Wang, X. Shan, Removal of cadmium from aqueous solutions by adsorption on granular red mud (GRM), Sep. Purif. Technol., 57 (2007) 161–169.
[4]   A.B. Pérez-Marín, V.M. Zapata, J.F. Ortuño, M. Aguilar, J. Sáez, M. Lloréns, Removal of cadmium from aqueous solutions by adsorption onto orange waste, J. Hazard. Mater., 139 (2007) 122–131.
[5]   M. Mahmood-Ul-Hassan, V. Suthor, E. Rafique, M. Yasin, Removal of Cd, Cr, and Pb from aqueous solution by unmodified and modified agricultural wastes, Environ. Monit. Assess., 187 (2015) 19.
[6]   N.C. Meng, J. Bo, C.W.K. Chow, C. Saint, Recent developments in photocatalytic water treatment technology: a review, Water Res., 44 (2010) 2997–3027.
[7]   R. Morsy, Synthesis and physicochemical evaluation of hydroxyapatite gel biosorbent for toxic Pb(II) removal from wastewater, Arabian J. Sci. Eng., 41 (2016) 2185–2191.
[8]   S. Bailliez, A. Nzihou, E. Beche, G. Flamant, Removal of lead (Pb) by hydroxyapatite sorbent, Process Saf. Environ. Prot., 82 (2004) 175–180.
[9]   K. Lin, C. Wu, J. Chang, Advances in synthesis of calcium phosphate crystals with controlled size and shape, Acta Biomater., 10 (2014) 4071–4102.
[10] D.X. Liao, W. Zheng, X.M. Li, Q. Yang, X. Yue, L. Guo, G. Zeng, Removal of lead(II) from aqueous solutions using carbonate

hydroxyapatite extracted from eggshell waste, J. Hazard. Mater., 177 (2010) 126–130.

[11] S.-D. Jiang, Q.-Z. Yao, G.-T. Zhou, S.-Q. Fu, Fabrication of hydroxyapatite hierarchical hollow microspheres and potential application in water treatment, J. Phys. Chem. C, 116 (2012) 4484–4492.

[12] X.-Y. Zhao, Y.-J. Zhu, J. Zhao, B.-Q. Lu, F. Chen, C. Qi, J. Wu, Hydroxyapatite nanosheet-assembled microspheres: hemoglobin-templated synthesis and adsorption for heavy metal ions, J. Colloid Interface Sci., 416 (2014) 11–18.

[13] F. Wang, Y. Guo, H. Wang, L. Yang, K. Wang, X. Ma, W. Yao, H. Zhang, Facile preparation of hydroxyapatite with a three dimensional architecture and potential application in water treatment, Cryst. Eng. Commun., 13 (2011) 5634–5637.

[14] Z. Zhang, M. Li, W. Chen, S. Zhu, N. Liu, L. Zhu, Immobilization of lead and cadmium from aqueous solution and contaminated sediment using nano-hydroxyapatite, Environ. Pollut., 158 (2010) 514–519.

[15] R.Z. Legeros, Calcium phosphate-based osteoinductive materials, Chem. Rev., 108 (2008) 4742–4753.

[16] L. Wang, G.H. Nancollas, Calcium orthophosphates: crystallization and dissolution, Chem. Rev., 108 (2008) 4628–4669.

[17] C. Qi, F. Chen, J. Wu, Y.-J. Zhu, C.-N. Hao, J.-L. Duan, Magnesium whitlockite hollow microspheres: a comparison of microwave-hydrothermal and conventional hydrothermal syntheses using fructose 1,6-bisphosphate, and application in protein adsorption, RSC Adv., 6 (2016) 33393–33402.

[18] C. Qi, Y.-J. Zhu, X.-Y. Zhao, B.-Q. Lu, Q.-L. Tang, J. Zhao, F. Chen, Highly stable amorphous calcium phosphate porous nanospheres: microwave-assisted rapid synthesis using ATP as phosphorus source and stabilizer, and their application in anticancer drug delivery, Chem. Eur. J., 19 (2013) 981–987.

[19] J. Zhao, Y.-J. Zhu, J. Wu, J.-Q. Zheng, X.-Y. Zhao, B.-Q. Lu, F. Chen, Chitosan-coated mesoporous microspheres of calcium silicate hydrate: environmentally friendly synthesis and application as a highly efficient adsorbent for heavy metal ions, J. Colloid Interface Sci., 418 (2014) 208–215.

[20] K. Lin, J. Pan, Y. Chen, R. Cheng, X. Xu, Study the adsorption of phenol from aqueous solution on hydroxyapatite nanopowders, J. Hazard. Mater., 161 (2009) 231–240.

[21] C. Qi, Y.-J. Zhu, B.-Q. Lu, G.-J. Ding, T.-W. Sun, F. Chen, J. Wu, Microwave-assisted rapid synthesis of magnesium phosphate hydrate nanosheets and their application in drug delivery and protein adsorption, J. Mater. Chem. B, 2 (2014) 8576–8586.

[22] J. Zhao, Y.-J. Zhu, J.-Q. Zheng, F. Chen, J. Wu, Microwave-assisted hydrothermal preparation using adenosine 5′-triphosphate disodium salt as a phosphate source and characterization of zinc-doped amorphous calcium phosphate mesoporous microspheres, Microporous Mesoporous Mater., 180 (2013) 79–85.

[23] L. Yang, W. Zhong, J. Cui, Z. Wei, W. Wei, Enhanced removal of Cu(II) ions from aqueous solution by poorly crystalline hydroxyapatite nanoparticles, J. Dispersion Sci. Technol., 37 (2015) 956–968.

[24] Y. Hashimoto, T. Sato, Removal of aqueous lead by poorly-crystalline hydroxyapatites, Chemosphere, 69 (2007) 1775–1782.

[25] W. Zhang, F.H. Wang, P.L. Wang, L. Lin, Y. Zhao, P. Zou, M.J. Zhao, H. Chen, Y. Liu, Y.S. Zhang, Facile synthesis of hydroxyapatite/yeast biomass composites and their adsorption behaviors for lead (II), J. Colloid Interface Sci., 477 (2016) 181–190.

[26] J. Cha, M. Cui, M. Jang, S.H. Cho, D.H. Moon, J. Khim, Kinetic and mechanism studies of the adsorption of lead onto waste cow bone powder (WCBP) surfaces, Environ. Geochem. Health, 33 (2011) 81–89.

[27] G.-J. Ding, Y.-J. Zhu, C. Qi, T.-W. Sun, J. Wu, F. Chen, Amorphous calcium phosphate nanowires prepared using beta-glycerophosphate disodium salt as an organic phosphate source by a microwave-assisted hydrothermal method and adsorption of heavy metals in water treatment, RSC Adv., 5 (2015) 40154–40162.

[28] G. Bharath, A.J. Kumar, K. Karthick, D. Mangalaraj, C. Viswanathan, N. Ponpandian, Shape evolution and size controlled synthesis of mesoporous hydroxyapatite nanostructures and their morphology dependent Pb(II) removal from waste water, RSC Adv., 4 (2014) 37446–37457.

[29] A.-R. Ibrahim, Y. Zhou, X. Li, L. Chen, Y. Hong, Y. Su, H. Wang, J. Li, Synthesis of rod-like hydroxyapatite with high surface area and pore volume from eggshells for effective adsorption of aqueous Pb(II), Mater. Res. Bull., 62 (2015) 132–141.

[30] X. Wen, C.-T. Shao, W. Chen, Y. Lei, Q.-F. Ke, Y.-P. Guo, Mesoporous carbonated hydroxyapatite/chitosan porous materials for removal of Pb(II) ions under flow conditions, RSC Adv., 6 (2016) 113940–113950.

[31] C.-Z. Zhang, Y. Yuan, Z. Guo, Experimental study on functional graphene oxide containing many primary amino groups fast-adsorbing heavy metal ions and adsorption mechanism, Sep. Sci. Technol., 53 (2018) 1666–1677.

[32] C.-Z. Zhang, B. Chen, Y. Bai, J. Xie, A new functionalized reduced graphene oxide adsorbent for removing heavy metal ions in water via coordination and ion exchange, Sep. Sci. Technol., 53 (2018) 2896–2905.

[33] C.-Z. Zhang, Y.-X. Su, M.-X. Niu, A selective chemosensor for detection of Ag(I) and Cu(I) based on an acenaphthoquinone derivative and its complexes, J. Coord. Chem., 69 (2016) 3158–3171.